analytical chemistry

pubs.acs.org/ac Article

Targeted Analysis of the Size Distribution of Heavy Chain-Modified Hyaluronan with Solid-State Nanopores

Dorothea A. Erxleben, Rebecca J. Dodd, Anthony J. Day, Dixy E. Green, Paul L. DeAngelis, Suruchi Poddar, Jan J. Enghild, Janet L. Huebner, Virginia B. Kraus, Amanda R. Watkins, Heidi L. Reesink, Elaheh Rahbar, and Adam R. Hall*

Cite This: https://doi.org/10.1021/acs.analchem.3c04387 Read Online

ACCESS | Metrics & More | Article Recommendations | Supporting Information

ABSTRACT: The glycosaminoglycan hyaluronan (HA) plays important roles in diverse physiological functions where the distribution of its molecular weight (MW) can influence its behavior and is known to change in response to disease conditions. During inflammation, HA undergoes a covalent modification in which heavy chain subunits of the inter-alpha-inhibitor family of proteins are transferred to its structure, forming heavy chain-HA (HC•HA) complexes. While limited assessments of HC•HA have been performed previously, determining the size distribution of its HA component remains a challenge. Here, we describe a selective method for extracting HC•HA from mixtures that yields material amenable to MW analysis with a solid-state nanopore sensor. After demonstrating the approach in vitro, we validate extraction of HC•HA from osteoarthritic human synovial fluid as a model complex biological matrix. Finally, we apply our technique to pathophysiology by measuring the size distributions of HC•HA and total HA in an equine model of synovitis.

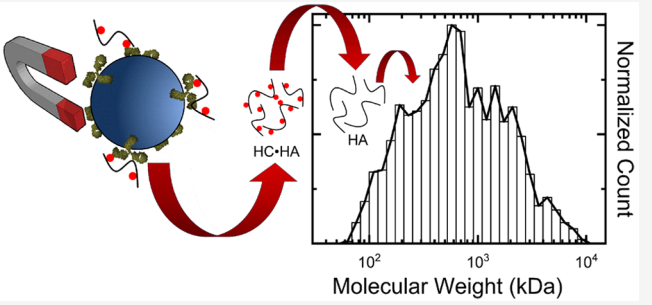

Hyaluronan[1,2] (HA) is an unbranched and nonsulfated glycosaminoglycan (GAG) that is composed of repeating disaccharides of D-glucuronic acid and *N*-acetyl-D-glucosamine (GlcNAcβ1-4GlcAβ1-3). Common to all vertebrates, the physiological roles of HA are guided by its molecular characteristics.[3] For example, HA helps to provide structure and hydration to the extracellular matrix, tissues, and joints[4−7] while its recognition by HA receptors contributes to leukocyte adhesion and intracellular signaling.[8] Another major driver of HA function is its molecular weight (MW), which has been reported to range dramatically from oligosaccharides to polymers MDa in size, averaging between 1 and 8 MDa in most vertebrates.[2,9] In humans, HA homeostasis is achieved through the balance of synthesis by hyaluronan synthases[10,11] (HAS1, HAS2, and HAS3) and degradation, including enzymatic degradation via hyaluronidases[7,12−14] (e.g., Hyal1, Hyal2, PH20, CEMIP, and TMEM2), that can turn over approximately one-third of the total HA in the human body daily.[15,16] Dysregulation of these pathways or other factors impacting the MW distribution of HA in tissues and biofluids can influence its function in vivo. For example, low MW forms of HA can act as competitive inhibitors[17] to high MW HA for receptor binding and promote pathological states. Consequently, HA has also been implicated in a number of diseases, including cancer where it is known to play a role in tumorigenesis and metastasis[18] due to its support of cell motility, proliferation (including cancer stem cell populations[19]), and inflammation.[4,20]

The biological functions of HA are also regulated by its interactions with hyaluronan-binding proteins.[21] Its recognition by cell surface receptors, including CD44 and LYVE-1, along with many other hyaladherins can be critical in guiding its physiological activity.[3,8,15,22] Notably, these interactions are noncovalent in nature, with the only known covalently complexed HA−protein interaction being with heavy chains (HCs) of the inter-alpha-inhibitor (IαI) family of proteoglycans.[23−25] In inflammatory conditions such as synovitis and arthritis,[26−28] and in some physiological processes (e.g., gut development,[29] ovulation,[30,31] and cervical ripening[32]), the upregulation of the secreted protein product of Tumor Necrosis Factor-Stimulated Gene-6 (TSG-6) enables HCs from IαI to transfer and attach covalently to the 6-OH groups of the N-acetylglucosamine residues of HA[30,33] to form HC•HA[24,34] (Figure 1a). Among many putative functions, HC•HA has been reported to stabilize HA matrices via cross-linking[24,25,28,35] and promote leukocyte adhesion.[36,37] In

Received: September 28, 2023
Revised: December 16, 2023
Accepted: December 18, 2023

https://doi.org/10.1021/acs.analchem.3c04387
Anal. Chem. XXXX, XXX, XXX−XXX

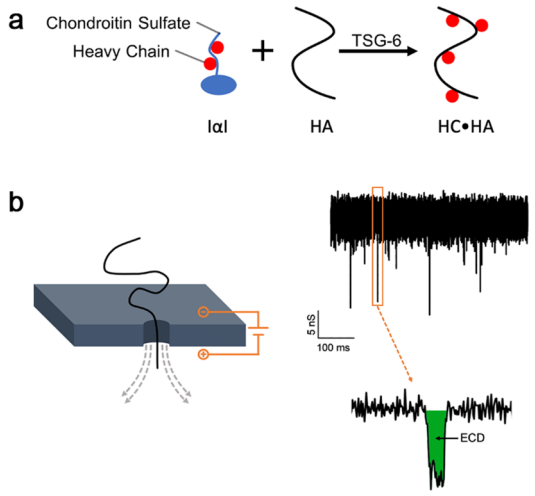

Figure 1. (a) Heavy chain transfer from IαI to HA occurs in the presence of TSG-6 to form HC•HA complexes. (b) HA is driven electrophoretically through an SSNP (left), producing a series of brief interruptions (events) in the nanopore conductance (upper right). The event area (event charge deficit or ECD, lower right) for each passing molecule is characteristic of molecular weight.

addition to displaying protective properties in some tissues and having therapeutic potential,[38,39] HC•HA has been implicated in disease processes such as acute lung injury,[40] airway hyperresponsiveness,[41] and rheumatoid arthritis,[27,28,36,42] although its precise roles in these contexts are still an area of active study.

While it has been suggested that high MW HA can receive and also donate HCs, the transfer of HCs to low MW HA is considered to be irreversible.[42] The precise role of HA MW in the functional activity of the complex is almost entirely unstudied, with very limited data on its size and composition. One notable exception is the work of Yingsung et al. which probed HA chains following the removal of HCs from the synovial fluid (SF) of patients with rheumatoid arthritis and reported that 3 to 5 HCs could associate with HA chains of approximately 2 MDa.[28] However, a more complete understanding of the HC•HA size distribution requires the direct determination of its MW profiles. Unfortunately, the technologies available for investigating the HC•HA size are limited. Both SDS-PAGE and Western blotting have been used to probe the complex, but with few exceptions[43] they only assess the HC component and in fact require digestion of HA in the process,[40,44] thereby restricting their capacity for investigating the glycan component. While agarose gel electrophoresis methods have been applied to the quantitative determination of HA MW,[43] their general requirement for significant sample amounts also creates a particular challenge in probing HC•HA that is likely to be in low abundance in most biofluids.[45] Enzyme-linked immunosorbent assays (ELISAs) have also been applied to HC•HA[46,47] but can only report on total concentration, yielding only a partial picture. To address a related sensitivity gap in total HA MW determination, we recently established a solid-state nanopore (SSNP) approach for analyzing HA with molecular precision.[48,49] Briefly, HA molecules are driven electrophoretically through a fabricated nanometer-scale pore under high ionic strength conditions. While transiting the pore, the presence of each HA molecule perturbs the measured ionic current in a manner that is characteristic of its individual size (Figure 1b). Consequently, analysis of several hundred or thousand representative HA molecules can deliver an MW distribution of an entire specimen from a very small sample mass (as little as ~10 ng) with single-molecule resolution. The SSNP approach has been applied to HA in a variety of complex biological matrices including bacterial glycocalyx,[50] bile ducts,[51] anterior axial tissues (anteroposterior AP axis),[52] ovarian tissues,[53] and equine SF,[54] but has so far not been applied specifically to HC•HA complexes.

Here, we extend SSNP analysis by incorporating an affinity-coupling technique capable of HC•HA extraction from mixed specimens with high selectivity. We first validate the basic concept using HC•HA constructs synthesized in vitro and then adapt our protocols to enable extraction from a complex biofluid using osteoarthritic human SF as a test matrix. Finally, we apply the approach to translational analysis by measuring the MW distributions of both HC•HA and HA in SF from an inflamed joint and a matched healthy contralateral joint in an equine model of synovitis. Our results demonstrate a new tool for probing HC•HA in biological matrices that will be valuable in studying its role in physiology, inflammation, and disease states.

MATERIALS AND METHODS

HA and HC•HA Samples. Quasi-monodisperse HA were synthesized chemoenzymatically as described previously[55] (Hyalose, LLC). HA MWs of 54, 81, 130, 237, 545, 1076, and 2384 kDa were used to compose SSNP calibration curves.[48] MW values were within 5% of the reported mean (polydispersity = 1.001−1.035, as estimated by size exclusion chromatography with multi-laser light scattering). The 237 and 545 kDa samples were employed for subsequent analyses. The 237 kDa HA was used to produce HC•HA via a transfer reaction[34] carried out by incubating 30 μg HA with 1.8 μM IαI (human serum-derived as described elsewhere[56]) and 0.28 μM rhTSG-6 (ref. 2104-TS, R&D Systems) for 20 h at 37 °C in a buffer of 20 mM HEPES, pH 7.4, 150 mM NaCl, and 5 mM $MgCl_2$ (100 μL final volume). To validate HC transfer, samples (typically 3 μL) from each reaction were analyzed by SDS-PAGE both with and without treatment with 1 U hyaluronidase from *Streptomyces hyaluronlyticus* (ref. 389561, Sigma-Aldrich) for 60 min at 37 °C to digest HA components. Enzyme-treated and control samples (incubated with an equivalent volume of water) were mixed 1:1 with 2× sample loading buffer (125 mM Tris base, pH 8.0, 87.5 mM SDS, 2 mM bromophenol blue, 3.125% (v/v) glycerol, 5% (v/v) β-mercaptoethanol) and incubated for 10 min at 80 °C before loading onto a 4−12% Bis-Tris SDS-PAGE gel (ref. NPO322, Invitrogen) and electrophoresed at 150 V for 2 h. Gels were stained with Ready Blue (ref. RSB, Sigma-Aldrich) for 4 h, then destained with water before imaging.

Affinity Extraction of HC•HA from *In Vitro* Mixtures. Superparamagnetic beads (Dynabeads M-270 Epoxy, ref. 14301, Thermo Fisher Scientific) were coupled with a rabbit polyclonal antibody raised against IαI (ref. A0301, Dako North America, Inc.) using an antibody coupling kit (Dynabeads Antibody Coupling Kit, ref. 14311D, Thermo Fisher Scientific) at a ratio of 5 μg of antibody ligand per 1 mg of beads and brought to a final coupled-bead concentration of 10 mg/mL. A sample containing HC•HA was then added to the antibody-beads and incubated at room temperature for at least 1 h. Beads with captured HC•HA were isolated under magnetic field, washed to remove unbound material, and resuspended in

https://doi.org/10.1021/acs.analchem.3c04387
Anal. Chem. XXXX, XXX, XXX−XXX

100 μL of phosphate buffered saline (PBS; 11.9 mM phosphates, 137 mM sodium chloride, and 2.7 mM potassium chloride, pH 7.4; ref. BP399, Thermo Fisher Scientific). A broad-range protease (Proteinase K, ref. AM2548, Invitrogen) was then added following manufacturer's directions to elute attached material and digest HCs simultaneously. An equal volume of phenol/chloroform/isoamyl alcohol, 25:24:1 (ref. 327111000, Thermo Fisher Scientific), was added to the sample, followed by thorough mixing and centrifugation (14000 × *g* for 15 min at 20 °C) in phase-lock gel tubes (ref. 2302830, QuantaBio) to partition the sample into an aqueous phase containing previously HC-bound constituent polysaccharides and an organic phase containing proteins and other byproducts of proteolysis. This procedure was carried out two more times with pure chloroform (ref. AC423555000, Thermo Fisher Scientific) to remove residual phenol. The aqueous fraction was then diluted with 10 M LiCl in 1X Tris-EDTA (10 mM Tris, 1 mM EDTA, pH 8.0; ref. BP1338, Thermo Fisher Scientific) to a final salt concentration of 6 M LiCl for subsequent SSNP measurements.

Human Synovial Fluid Collection. Human knee OA SF was aspirated as part of standard care and stored as anonymous "waste" material under a protocol approval by the Duke IRB (Pro00008622). The sample was processed within 4 h of collection by centrifugation at 1000−2000 × *g* at 4 C for 15 min. The supernatant was stored at −80 °C until analysis. The human SF specimen used for this study was from a 72-year-old black female patient who had recurrent effusion after having received an intra-articular steroid injection 6 months prior.

Equine Synovitis Model Synovial Fluid Collection. SF samples were obtained as previously described[57] with protocol approval by the Cornell University IACUC (#2018-0024). Briefly a 20-year-old Mustang/Arabian cross mare was evaluated by 2 veterinarians and determined to have no pre-existing lameness or joint effusion. A total of 100 ng of recombinant equine IL-1ß (Novus Biologicals) in 1 mL of PBS was administered intra-articularly into a randomly assigned middle carpal joint (to induce synovitis), while the contralateral middle carpal joint was injected with 1 mL of PBS (contralateral control). Three mL of SF were collected from both joints 12 h after IL-1ß injection. Samples were processed within 2 h of collection by centrifugation at 4000 × *g* at 4 °C for 15 min, followed by storage of frozen supernatant at −80 °C until analysis.

Affinity Extraction of HA from Synovial Fluid. HA was extracted following general protocols reported previously[48] with some modifications. Briefly, biological samples (5 μL for human SF, 25 μL for equine SF) underwent a buffer exchange into 1× PBS using an ultrafiltration device (3 kDa cutoff Amicon Ultra, ref. UFC5003, Millipore Sigma). Broad-range protease treatment followed by solvent extractions and washes was then carried out as described above to partition samples into an aqueous phase containing HA, nucleic acids, and other polysaccharides and an organic phase containing proteins and other byproducts of proteolysis. HA was then captured and extracted from the aqueous fraction by biomagnetic precipitation using recombinant versican G1 (VG1) domain[58] to bind HA on superparamagnetic beads ("VG1-beads"). For this, streptavidin-conjugated superparamagnetic beads (Dynabeads M-280 Streptavidin, ref. 11206D, Thermo Fisher Scientific) were first washed according to the manufacturer's directions and then incubated for 1 h at room temperature with biotinylated VG1 (bVG1, ref. G-HA02, Echelon Biosciences) at a ratio of 1 μg bVG1 per 100 μg of beads in 1X PBS. The resulting VG1-beads were washed thoroughly and resuspended into 150 μL aliquots at a concentration of 10 mg/mL in 1X PBS. An aqueous sample containing HA was added to an aliquot of beads stepwise to avoid MW bias in the capture and incubated at room temperature for at least 1 h. HA-bound beads were isolated with a magnet and washed to remove the unbound material. Beads were then incubated with 50 μL of SSNP measurement buffer (6 M LiCl in 1X Tris-EDTA) for 1 h, wherein the high ionic strength disrupted the HA-VG1 interaction to elute HA.

Affinity Extraction of HC•HA from Synovial Fluid. Biological samples (5 μL for human SF, 100 μL for equine SF) underwent a buffer exchange into 1× PBS using ultrafiltration devices. Sample was then added to antibody-beads stepwise to avoid biased capture dynamics and incubated at room temperature for at least 1 h. Beads with captured HC•HA were isolated under magnetic field, washed to remove unbound material, and resuspended in 50 μL (for human samples) or 100 μL (for equine samples) of 1× PBS. Broad-range protease treatment followed by solvent extractions and washes was then carried out as described above to elute attached material from the antibody-beads and digest HCs simultaneously. The solvent-extracted aqueous samples underwent an additional purification of HA using VG1-beads, as described above, to remove potential polysaccharide (e.g., CS) contaminants.

SSNP Measurements and Analyses. SSNPs consisting of a single pore in a 20−30 nm thick low stress silicon nitride membrane were fabricated using either a Helium ion milling method reported previously,[59] or obtained commercially (Norcada, Inc.). All pores displayed a linear current−voltage curve with a resistance that yielded a diameter in the range of 6.3−11.6 nm as calculated from an established model[60] that assumed an effective pore thickness of 1/3 membrane thickness. Each device was rinsed with ethanol and water, dried with filtered air, and then treated with air plasma (30 W, Harrick Plasma) for at least 2 min per side before being mounted into a custom 3D-printed flow cell (Carbon, Inc.). Measurement buffer (6 M LiCl, 10 mM Tris, and 1 mM EDTA, pH 8.0) was introduced to the flow cells to contact each side of the nanopore membrane. Ag/AgCl electrodes were connected to a patch-clamp amplifier (Axopatch 200B, Molecular Devices) and used to both apply voltage and measure current. For HA measurements, isolated HA samples suspended in 10 μL of a 6 M LiCl SSNP measurement buffer were loaded on one side of the pore. A 200 to 300 mV bias was then applied, and the transmembrane current was monitored at a rate of 200 kHz using a 100 kHz four-pole Bessel filter. Data were collected and analyzed by using a custom LabVIEW program (National Instruments). An additional 5 kHz low-pass filter was applied during analysis. Molecular translocations were marked by temporary reductions in the ionic current events and analyzed using thresholds of 5 standard deviations of the root-mean-square noise.[49] The magnitude of each event (i.e., the integrated area dependent on translocation dwell time and amplitude of measured conductance) was correlated to its corresponding MW using calibration curves produced by measuring quasi-monodisperse samples of HA with known MWs (see HA and HC•HA Samples) and calculating their corresponding average ECD values as described previously.[48] Events with ECD values corresponding to MWs between 50 kDa and 10 MDa based on calibrations were considered in the analysis.

https://doi.org/10.1021/acs.analchem.3c04387
Anal. Chem. XXXX, XXX, XXX−XXX

RESULTS AND DISCUSSION

SSNP measurements are not intrinsically selective in that all molecules with appropriate charge can be translocated by the applied electric field and potentially produce characteristic signals ("events"). As a result, studying any specific biomolecule from a mixture requires either the accurate identification and differentiation of mixed signals,[61,62] the implementation of a specialized assay to provide selectivity,[63,64] or the deployment of a sample pretreatment designed to sequester only the target molecules for further study. Because of the challenges associated with applying the former two approaches to HA, we have previously used an affinity extraction protocol in our analyses of this GAG.[48] This extraction relied on HA-specific VG1-beads that can then be pulled down to remove other background molecules. While captured HA molecules should, in principle, include those with covalently bound HCs, an initial broad-spectrum protease step used to digest hyaladherins from the complex milieu would render them indistinguishable from unmodified material.

Toward extending our analyses to HC•HA, we first modified our extant extraction protocol to target the HCs themselves by incorporating superparamagnetic beads coupled with rabbit polyclonal antibodies raised against IαI isolated from human serum (Figure 2a). In support of this development, we produced a mixture of two quasi-monodisperse HA samples: one unmodified HA with an average MW of 545 kDa and the other an HA with an average MW of 237 kDa and conjugated with HC *in vitro* through incubation with IαI and TSG-6[34] (Figure 2b; see Materials and Methods). SSNP size analysis of the mixture, following a simple protease treatment to remove all bound HCs, yielded two discrete populations at the expected sizes (Figure 2c, top). We then captured HC•HA specifically from the mixture by introducing antibody-beads. After precipitating the beads magnetically and removing the supernatant, they were washed to remove any material bound nonspecifically and were treated with a broad-spectrum protease to digest both the antibodies and the HCs, resulting in eluted HA that solely represented the glycan component of the HC•HA population (Figure 2c, bottom). Following this immunomagnetic extraction protocol, SSNP analysis yielded a single peak at 237 kDa, corresponding to the HC•HA population alone. No significant events were observed at the 545 kDa level, confirming both the lack of nonspecific capture and the selectively of the extraction.

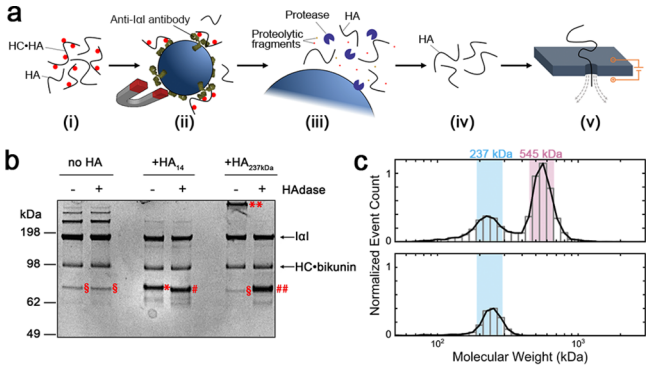

Figure 2. (a) Schematic illustrating the HC•HA extraction protocol: a synthetic mixture (*i*) of HA and HC•HA (HCs shown as red circles) is incubated with antibody-beads (*ii*) to capture HC•HAs and extract them magnetically. Beads are protease-treated to digest HCs (*iii*) and release pure HA (*iv*) for subsequent SSNP analysis (*v*). (b) Validation of HC•HA formed in vitro via SDS-PAGE. Lanes feature equal volumes of HC•HA reaction mixtures, including "no HA" (IαI and TSG-6 only; negative control), "+HA_{14}" (positive control) or "+HA_{237kDa}" (experimental condition), each treated with and without *Streptomyces hyaluronidase* (HAdase) to digest HA and analyzed by SDS-PAGE under reducing conditions. Positions of IαI and HC•bikunin are indicated with arrows. Free HC is denoted by §. The covalent complex formed between HA_{14} and HC (HC•HA_{14}) is denoted by * and the HC (with an HA "stub") released from this complex by HAdase by #. The covalent complex formed between HA_{237kDa} and HC (HC•HA_{237kDa}) is denoted by ** and the HC (with an HA "stub") released from this complex by HAdase by ##. TSG-6 (~35 kDa) is not visible on the gel since it is present in the reactions at a catalytic concentration. (c) MW distribution histograms derived from SSNP analyses of (top) a synthetic mixture of monodisperse HC•HA (237 kDa, light blue shaded region) and HA (545 kDa, light red shaded region) and (bottom) the extracted population (237 kDa). Numbers of events: 10588 (top); 1481 (bottom).

Having established a fundamental ability to capture and elute HC•HA, we next applied the approach to a complex biofluid. As a model, we used human SF collected from the knee joint of a subject with osteoarthritis (OA). SF is known to contain an abundance of HA in general[9] and OA SF was used specifically to provide a robust population of HC•HA complexes as was shown previously to be associated with the disease.[27,65] To validate the utility of our extraction procedure for capturing this HC•HA, we first spiked OA SF with the 237 kDa HC•HA made *in vitro* (as described above) and performed an identical extraction process. While SSNP signals were measured for the sample following extraction, the MW distribution derived from these data (Figure 3a) did not yield

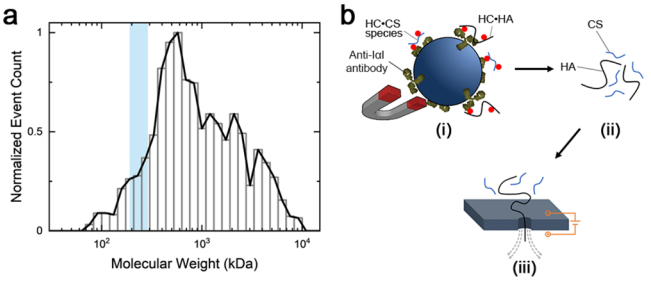

Figure 3. (a) MW distribution histogram derived from SSNP analysis of HC•HA extracted from human OA SF with a 237 kDa spike-in using the initial extraction protocol. Light blue shaded region denotes the expected 237 kDa spike-in recovery. No peak was observed. Number of events: 1332. (b) Schematic illustrating competitive capture of HC•HA and HC•CS species (*i*), resulting in CS contamination in the extracted HA (*ii*), and subsequent unintentional detection by SSNP (*iii*).

the anticipated spike-in peak at 237 kDa. This observation called into question the origin of the observed signals and suggested the possibility of some form of background interference unique to the SF biological matrix. It was not immediately clear what could account for this background, since other protein constituents of the SF are digested by the protease treatment component of the extraction process. However, an explanation was identified in the presence of off-target proteoglycans.

The anti-IαI antibody used to capture HC•HA would also extract IαI itself as well as related molecules such as pre-alpha-inhibitor (PαI), which contains a chondroitin sulfate (CS) chain attached to a single HC.[25] Additionally, HCs can be

https://doi.org/10.1021/acs.analchem.3c04387
Anal. Chem. XXXX, XXX, XXX−XXX

transferred to CS chains with regions of low sulfation[66] in a variety of proteoglycans[67,68] including possibly fragments of aggrecan that are known to be present in OA SF.[69] Consequently, a protease treatment of antibody-captured material would also release interfering glycans (e.g., CS) that are potentially capable of being translocated through the SSNP under the same applied voltage as that of HA (Figure 3b). While the CS associated with proteoglycans can vary in both chain length[70,71] and degree of sulfation,[72,73] CS translocation dynamics through nanopores are almost[74] entirely unstudied and the nonhomogeneous charge resulting from their variable sulfation may enable detection of smaller molecules than the threshold that applies to HA. Indeed, we independently subjected IαI alone to a protease treatment and then performed SSNP analysis to test this concept. We found that what remained after digestion produced significant events on its own (Supporting Information, Figure S1), suggesting that residual CS could have contributed to some fraction of the signals detected from the OA SF.

To address this challenge, we next sought to modify our extraction protocol to better target HC•HA alone. A possible solution was to digest the remnant CS to leave only HA for analysis, but CS enzymes have been reported to also degrade HA.[75−77] Alternatively, we reasoned that an extraction with VG1-beads recognizing HA could be performed in addition to the procedure described above to select only for HC•HA (Figure 4a). Therefore, after protease elution from the antibody-beads and subsequent cleanup, eluted material derived from spiked OA SF was reintroduced to a second set of superparamagnetic beads with VG1 attached. Following binding, washing, and elution with high-molarity salt solution (see Materials and Methods), pure HA material was collected and analyzed via SSNP. Despite the limitations of overall bead capacity and the unknown amount of captured HC•HA, this double-extraction approach provided sufficient material to enable robust detection of events (typical event rates ∼1.2 s^{-1}) and construction of MW distributions from the resulting data. With the improved extraction protocol, we observed a clear peak at 237 kDa for the spiked OA SF specimen, indicating that interfering molecules (e.g., CS) had indeed been removed. Consequently, the background distribution of the spiked OA SF as well as that obtained from the native OA SF sample could provide a MW assessment of HA molecules that had been decorated with one or more HCs in the biofluid (Figure 4b, left).

For comparison, we also performed analyses of the OA SF following isolation with only VG1-beads, thereby targeting all of the HA present in the specimen. The spiked sample again revealed a peak at the expected position of 237 kDa (Figure 4b, right), although less pronounced than in the case of HC•HA extraction, likely reflecting the larger abundance of total HA (both with and without attached HCs) in the sample relative to the spike. Notably, we found that the MW distribution of total HA matched closely with that of the HC•HA in the native specimen (Supporting Information, Figure S2). This observation suggested no significant preference toward a particular HA size range in the transfer of HCs by TSG-6, consistent with conclusions from previous biochemical studies.[34]

Finally, we used our approach to compare HA and HC•HA between paired equine SF samples obtained from a joint with experimentally induced synovitis and a paired, contralateral healthy control joint. This model was selected to overcome the

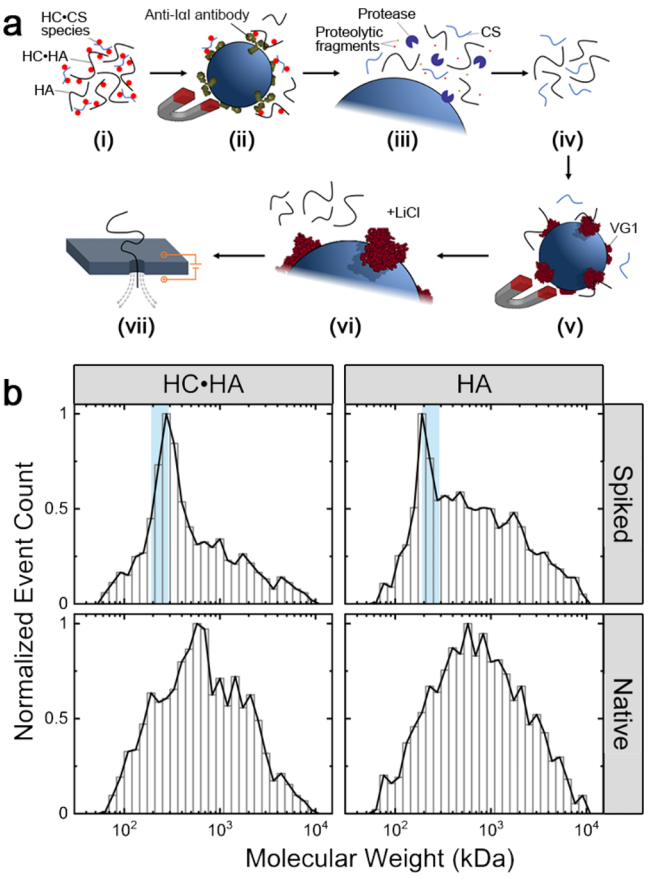

Figure 4. Recovery of spiked-in HC•HA from a complex biofluid (human OA SF). (a) Schematic illustrating the complete HC•HA extraction protocol. Complex fluid (*i*) is incubated with antibody-beads to pull down HC•HA and other HC•CS species magnetically (*ii*). A protease treatment (*iii*) digests HCs and antibodies to release HA and CS (*iv*), which are subsequently incubated with VG1-beads (*v*) to capture and pull HA down selectively. High-molarity LiCl is used to disrupt HA-VG1 and elute HA (*vi*) for SSNP analysis (*vii*). (b) MW distribution histograms derived from SSNP analyses of (top) spiked HC•HA and HA samples with shaded light blue region denoting the expected 237 kDa spike-in recovery and (bottom) native HC•HA and HA samples (no spike-in). Numbers of events: 1630 (upper left), 1665 (upper right), 1340 (lower left), and 1355 (lower right).

challenge of obtaining healthy human SF as a counterpoint to human OA SF. The equine carpal synovitis model is well-established as a representation of early OA pathogenesis that enables repeated arthrocentesis of sufficient SF volume for biochemical analyses.[78−81] Because this model employs an IL-1β injection to induce synovitis in a single forelimb, the contralateral limb provides a paired healthy control. Notably, the anti-IαI antibody utilized here has been validated to recognize equine isoforms of HC.[54] We first extracted and analyzed total HA from both SF specimens (Figure 5, left) and found that median MW in the synovitis SF was significantly lower (median 311 kDa, IQR 133−1118 kDa) than in the contralateral healthy SF (median 439 kDa, IQR 151−1940 kDa). This shift coincides with the known reduction of HA size distribution in OA[82] and is in accordance with previous data on the same model system wherein a specific loss in high MW HA following induction was reported.[57] Performing the analysis for HC•HA from the same specimens (Figure 5, right), a similar trend was observed wherein the size

https://doi.org/10.1021/acs.analchem.3c04387
Anal. Chem. XXXX, XXX, XXX−XXX

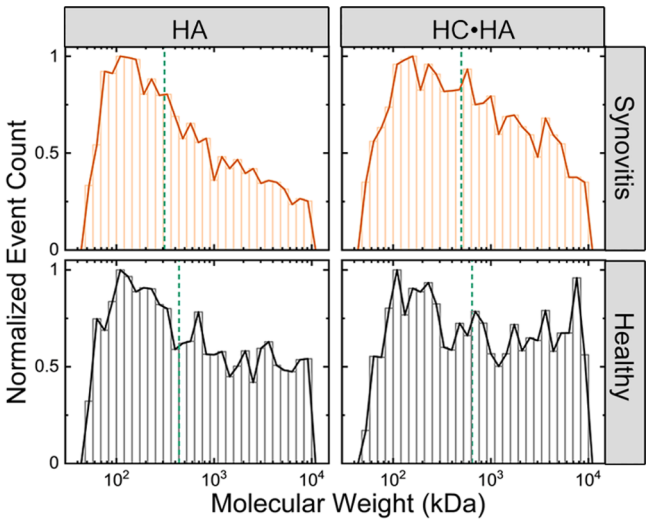

Figure 5. MW distribution histograms derived from two separate SSNP analyses each of (left) native HA and (right) native HC•HA in a (top) synovitis joint 12 h postinduction and a (bottom) contralateral healthy joint. Dashed vertical lines indicate median values. Independent distributions were weighted equally in analysis.

distribution shifted toward lower MW in the synovitis SF (median 498 kDa, IQR 172−1660 kDa) compared to the contralateral healthy SF (median 642 kDa, IQR 186−2718 kDa). Each distribution comprised two measurements on independent SSNP devices (Supporting Information, Figure S4), weighted equally in the analysis. The comparable shifts to smaller sizes of both HC•HA and total HA in the synovitis SF relative to those in the contralateral healthy SF could again suggest a lack of MW preference for HC attachment. However, under both conditions we observed a lower correspondence between the distributions of HC•HA and HA than was observed in the human OA SF measurements (c.f., Figure 4b). Further measurements will be needed to determine whether these differences are statistically robust for this model.

CONCLUSIONS

Herein we report a bead-based immunomagnetic technique capable of extracting HC•HA that can subsequently be analyzed by SSNP to yield a MW distribution of its HA constituent. We first used *in vitro* mixtures of size defined HA (545 kDa) and HC•HA (237 kDa) to demonstrate selective retention and detection of the latter when an anti-IαI antibody was used for capture. We found no significant nonspecific interactions with this protocol. We then applied the approach to biofluids by examining human OA SF, but observed interference in the analysis signals that were associated with the abundance of non-HA HC-bearing species present in the complex matrix. To overcome this, we modified the approach to include a secondary extraction, enabling better targeting of HC•HA components alone. Analysis of the resulting material yielded a size distribution of native HC•HA that was found to match closely with that of total HA (i.e., both with and without HC modification). Finally, we used our validated protocol to probe SF from an equine model that provided one joint with an IL-1β-induced synovitis phenotype emulating early stage OA and a contralateral joint operating as a healthy control. We showed that the size distributions of both HC•HA and total HA shifted toward lower MW in the synovitis joint relative to the control, in accordance with the inflammatory nature of the disease.

Overall, our extraction methodology provides a route for SSNP analysis to be applied specifically to the MW determination of HC•HA in physiological biofluids. Combined with the extant capabilities of the platform for measuring total HA MW distribution, this added functionality will enable a more complete assessment of the interplay between HC•HA and HA in healthy and pathological processes.

ASSOCIATED CONTENT

Supporting Information

The Supporting Information is available free of charge at https://pubs.acs.org/doi/10.1021/acs.analchem.3c04387.

Supplemental method for the analysis of protease-digested IαI with accompanying plot, a coplot of MW distributions of HC•HA and HA recovered from human OA SF with and without spike-in, and independent measurements of equine HC•HA and HA taken on multiple SSNPs (PDF)

AUTHOR INFORMATION

Corresponding Author

Adam R. Hall − *Virginia Tech-Wake Forest University School of Biomedical Engineering and Sciences, Wake Forest School of Medicine, Winston-Salem, North Carolina 27101, United States; Comprehensive Cancer Center, Wake Forest School of Medicine, Winston-Salem, North Carolina 27157, United States;* orcid.org/0000-0003-2053-6075; Email: arhall@wakehealth.edu

Authors

Dorothea A. Erxleben − *Virginia Tech-Wake Forest University School of Biomedical Engineering and Sciences, Wake Forest School of Medicine, Winston-Salem, North Carolina 27101, United States*

Rebecca J. Dodd − *Wellcome Centre for Cell-Matrix Research, Faculty of Biology, Medicine and Health, Manchester Academic Health Science Centre, University of Manchester, Manchester M13 9PT, United Kingdom*

Anthony J. Day − *Wellcome Centre for Cell-Matrix Research, Faculty of Biology, Medicine and Health, Manchester Academic Health Science Centre, University of Manchester, Manchester M13 9PT, United Kingdom; Lydia Becker Institute of Immunology and Inflammation, Faculty of Biology, Medicine and Health, Manchester Academic Health Science Centre, University of Manchester, Manchester M13 9PL, United Kingdom*

Dixy E. Green − *Department of Biochemistry and Molecular Biology, University of Oklahoma Health Sciences Center, Oklahoma City, Oklahoma 73104, United States*

Paul L. DeAngelis − *Department of Biochemistry and Molecular Biology, University of Oklahoma Health Sciences Center, Oklahoma City, Oklahoma 73104, United States*

Suruchi Poddar − *Virginia Tech-Wake Forest University School of Biomedical Engineering and Sciences, Wake Forest School of Medicine, Winston-Salem, North Carolina 27101, United States*

Jan J. Enghild − *Department of Molecular Biology and Genetics, Aarhus University, Aarhus C 8000, Denmark*

https://doi.org/10.1021/acs.analchem.3c04387
Anal. Chem. XXXX, XXX, XXX−XXX

Janet L. Huebner − *Duke Molecular Physiology Institute and Department of Medicine, Duke University School of Medicine, Durham, North Carolina 27710, United States*
Virginia B. Kraus − *Duke Molecular Physiology Institute and Department of Medicine, Duke University School of Medicine, Durham, North Carolina 27710, United States*
Amanda R. Watkins − *Department of Clinical Sciences, College of Veterinary Medicine, Cornell University, Ithaca, New York 14853, United States*
Heidi L. Reesink − *Department of Clinical Sciences, College of Veterinary Medicine, Cornell University, Ithaca, New York 14853, United States*
Elaheh Rahbar − *Virginia Tech-Wake Forest University School of Biomedical Engineering and Sciences, Wake Forest School of Medicine, Winston-Salem, North Carolina 27101, United States*

Complete contact information is available at: https://pubs.acs.org/10.1021/acs.analchem.3c04387

Author Contributions

D.A.E. performed extractions and nanopore measurements, analyzed the data, contributed to experimental design, and wrote the manuscript. R.J.D. and A.J.D. produced and validated the HC•HA material and contributed to experimental design. D.E.G. synthesized quasi-monodisperse HA material. P.L.D. synthesized quasi-monodisperse HA material and contributed to experimental design. S.P. contributed to extractions and nanopore measurements of equine SF samples. J.J.E. provided human serum-derived IαI. J.L.H. and V.B.K. provided the human OA SF specimen. A.R.W. and H.L.R. provided the equine SF biospecimens. E.R. contributed to the experimental design. A.R.H. oversaw the project, contributed to experimental design, and wrote the manuscript. All authors contributed to the editing and review of the manuscript.

Notes

The authors declare the following competing financial interest(s): A.R.H., P.L.D., and E.R. are listed as inventors on a patent covering SSNP analysis of hyaluronan. P.L.D. receives royalties from Hyalose, LLC product sales. A.J.D. is a founder of Link Biologics Limited, that is developing a TSG-6-based biological drug (Link_TSG6), and A.J.D. and R.J.D. are shareholders in the company; this is unconnected with the work described in this paper.

■ ACKNOWLEDGMENTS

This work was supported by the National Institutes of Health (NIH) Grants R01 GM134226 (to A.R.H. and E.R.), P41 EB020594 (to A.R.H.), K25 HL133611 (to E.R.), and P30 AG028716 (to V.B.K. and J.L.H.), Versus Arthritis Grant 22277 (to A.J.D.), and partial support from the Oklahoma Center for Advancement of Science and Technology (OCAST) Grant HR18-104 (to P.L.D.). B.D. gratefully acknowledges support from the Wellcome Centre for Cell-Matrix through its core funding from Wellcome Grants 203128/Z/16/Z and 220926/Z/20/Z (to A.J.D.). The authors thank Vincent Hascall (Cleveland Clinic) for providing the Dako antibody and Ian Wadsworth for additional protein analysis.

■ REFERENCES

(1) Meyer, K.; Palmer, J. W. *J. Biol. Chem.* **1934**, *107* (3), 629−634.
(2) Necas, J.; Bartosikova, L.; Brauner, P.; Kolar, J. *Vet Med-Czech* **2008**, *53* (8), 397−411.
(3) Richter, R. P.; Baranova, N. S.; Day, A. J.; Kwok, J. C. *Curr. Opin. Struct. Biol.* **2018**, *50*, 65−74.
(4) Abatangelo, G.; Vindigni, V.; Avruscio, G.; Pandis, L.; Brun, P. *Cells* **2020**, *9* (7), 1743.
(5) Zhu, L.; Seror, J.; Day, A. J.; Kampf, N.; Klein, J. *Acta Biomater.* **2017**, *59*, 283−292.
(6) Seror, J.; Zhu, L.; Goldberg, R.; Day, A. J.; Klein, J. *Nat. Commun.* **2015**, *6* (1), 6497.
(7) Dicker, K. T.; Gurski, L. A.; Pradhan-Bhatt, S.; Witt, R. L.; Farach-Carson, M. C.; Jia, X. *Acta Biomater.* **2014**, *10* (4), 1558−1570.
(8) Johnson, L. A.; Jackson, D. G. *Cells* **2021**, *10* (8), 2061.
(9) Cowman, M. K.; Lee, H.-G.; Schwertfeger, K. L.; McCarthy, J. B.; Turley, E. A. *Front. Immunol.* **2015**, *6*, na.
(10) Maloney, F. P.; Kuklewicz, J.; Corey, R. A.; Bi, Y.; Ho, R.; Mateusiak, L.; Pardon, E.; Steyaert, J.; Stansfeld, P. J.; Zimmer, J. *Nature* **2022**, *604* (7904), 195−201.
(11) Weigel, P. H. *Int. J. Cell Biol.* **2015**, *2015*, 1−15.
(12) Spataro, S.; Guerra, C.; Cavalli, A.; Sgrignani, J.; Sleeman, J.; Poulain, L.; Boland, A.; Scapozza, L.; Moll, S.; Prunotto, M. *FEBS J.* **2023**, *290* (16), 3946−3962.
(13) Domanegg, K.; Sleeman, J. P.; Schmaus, A. *Cancers* **2022**, *14* (20), 5093.
(14) Narita, T.; Tobisawa, Y.; Bobkov, A.; Jackson, M.; Ohyama, C.; Irie, F.; Yamaguchi, Y. *J. Biol. Chem.* **2023**, *299* (9), No. 105120.
(15) Jackson, D. G. *Immunol. Rev.* **2009**, *230* (1), 216−231.
(16) Fraser, J. R. E.; Laurent, T. C.; Laurent, U. B. G. *J. Int. Med.* **1997**, *242* (1), 27−33.
(17) Curk, T.; Dubacheva, G. V.; Brisson, A. R.; Richter, R. P. *J. Am. Chem. Soc.* **2022**, *144* (38), 17346−17350.
(18) Tammi, M. I.; Oikari, S.; Pasonen-Seppänen, S.; Rilla, K.; Auvinen, P.; Tammi, R. H. *Matrix Biol.* **2019**, *78*−*79*, 147−164.
(19) Price, Z.; Lokman, N.; Ricciardelli, C. *Cancers* **2018**, *10* (12), 482.
(20) Kobayashi, T.; Chanmee, T.; Itano, N. *Biomolecules* **2020**, *10* (11), 1525.
(21) Day, A. J.; Prestwich, G. D. *J. Biol. Chem.* **2002**, *277* (7), 4585−4588.
(22) Carvalho, A. M.; Reis, R. L.; Pashkuleva, I. *Adv. Healthc. Mater.* **2023**, *12* (5), No. 2202118.
(23) Bost, F.; Diarra-Mehrpour, M.; Martin, J.-P. *Eur. J. Biochem.* **1998**, *252* (3), 339−346.
(24) Day, A. J.; Milner, C. M. *Matrix Biol.* **2019**, *78*−*79*, 60−83.
(25) Lord, M. S.; Melrose, J.; Day, A. J.; Whitelock, J. M. *J. Histochem. Cytochem.* **2020**, *68* (12), 907−927.
(26) Chou, C.-H.; Attarian, D. E.; Wisniewski, H.-G.; Band, P. A.; Kraus, V. B. *Osteoarthritis Cartilage* **2018**, *26* (2), 245−254.
(27) Kida, D.; Yoneda, M.; Miyaura, S.; Ishimaru, T.; Yoshida, Y.; Ito, T.; Ishiguro, N.; Iwata, H.; Kimata, K. *J. Rheumatol.* **1999**, *26* (6), 1230−1238.
(28) Yingsung, W.; Zhuo, L.; Mörgelin, M.; Yoneda, M.; Kida, D.; Watanabe, H.; Ishiguro, N.; Iwata, H.; Kimata, K. *J. Biol. Chem.* **2003**, *278* (35), 32710−32718.
(29) Sivakumar, A.; Mahadevan, A.; Lauer, M. E.; Narvaez, R. J.; Ramesh, S.; Demler, C. M.; Souchet, N. R.; Hascall, V. C.; Midura, R. J.; Garantziotis, S.; Frank, D. B.; Kimata, K.; Kurpios, N. A. *Dev. Cell* **2018**, *46* (5), 533.
(30) Briggs, D. C.; Birchenough, H. L.; Ali, T.; Rugg, M. S.; Waltho, J. P.; Ievoli, E.; Jowitt, T. A.; Enghild, J. J.; Richter, R. P.; Salustri, A.; Milner, C. M.; Day, A. J. *J. Biol. Chem.* **2015**, *290* (48), 28708−28723.
(31) Zhuo, L.; Yoneda, M.; Zhao, M.; Yingsung, W.; Yoshida, N.; Kitagawa, Y.; Kawamura, K.; Suzuki, T.; Kimata, K. *J. Biol. Chem.* **2001**, *276* (11), 7693−7696.
(32) Kishida, T.; Yabushita, H.; Wakatsuki, A.; Zhuo, L.; Kimata, K. *Connect. Tissue Res.* **2008**, *49* (2), 105−108.
(33) Zhao, M.; Yoneda, M.; Ohashi, Y.; Kurono, S.; Iwata, H.; Ohnuki, Y.; Kimata, K. *J. Biol. Chem.* **1995**, *270* (44), 26657−26663.

(34) Rugg, M. S.; Willis, A. C.; Mukhopadhyay, D.; Hascall, V. C.; Fries, E.; Fülöp, C.; Milner, C. M.; Day, A. J. *J. Biol. Chem.* **2005**, *280* (27), 25674−25686.
(35) Baranova, N. S.; Inforzato, A.; Briggs, D. C.; Tilakaratna, V.; Enghild, J. J.; Thakar, D.; Milner, C. M.; Day, A. J.; Richter, R. P. *J. Biol. Chem.* **2014**, *289* (44), 30481−30498.
(36) Zhuo, L.; Kanamori, A.; Kannagi, R.; Itano, N.; Wu, J.; Hamaguchi, M.; Ishiguro, N.; Kimata, K. *J. Biol. Chem.* **2006**, *281* (29), 20303−20314.
(37) Baranova, N. S.; Foulcer, S. J.; Briggs, D. C.; Tilakaratna, V.; Enghild, J. J.; Milner, C. M.; Day, A. J.; Richter, R. P. *J. Biol. Chem.* **2013**, *288* (41), 29642−29653.
(38) Tseng, S. C. G. *Invest. Ophthalmol. Vis. Sci.* **2016**, *57* (5), ORSFh1.
(39) Zhu, Y.-T.; Li, F.; Zhang, Y.; Chen, S.-Y.; Tighe, S.; Lin, S.-Y.; Tseng, S. C. G. *Invest. Ophthalmol. Vis. Sci.* **2020**, *61* (5), 62.
(40) Ni, K.; Gill, A.; Tseng, V.; Mikosz, A. M.; Koike, K.; Beatman, E. L.; Xu, C. Y.; Cao, D.; Gally, F.; Mould, K. J.; Serban, K. A.; Schweitzer, K. S.; March, K. L.; Janssen, W. J.; Nozik-Grayck, E.; Garantziotis, S.; Petrache, I. *Respiratory Res.* **2018**, *19*, 107.
(41) Stober, V. P.; Johnson, C. G.; Majors, A.; Lauer, M. E.; Cali, V.; Midura, R. J.; Wisniewski, H.-G.; Aronica, M. A.; Garantziotis, S. *J. Biol. Chem.* **2017**, *292* (51), 20845−20858.
(42) Lauer, M. E.; Glant, T. T.; Mikecz, K.; DeAngelis, P. L.; Haller, F. M.; Husni, M. E.; Hascall, V. C.; Calabro, A. *J. Biol. Chem.* **2013**, *288* (1), 205−214.
(43) He, H.; Li, W.; Tseng, D. Y.; Zhang, S.; Chen, S.-Y.; Day, A. J.; Tseng, S. C. G. *J. Biol. Chem.* **2009**, *284* (30), 20136−20146.
(44) Lauer, M. E.; Loftis, J.; de la Motte, C.; Hascall, V. C. Analysis of the Heavy-Chain Modification and TSG-6 Activity in Pathological Hyaluronan Matrices. In *Glycosaminoglycans*; Balagurunathan, K., Nakato, H., Desai, U. R., Eds.; Methods in Molecular Biology; Springer New York: New York, NY, 2015; Vol. *1229*, pp 543−548.
(45) Rivas, F.; Erxleben, D.; Smith, I.; Rahbar, E.; DeAngelis, P. L.; Cowman, M. K.; Hall, A. R. *Am. J. Physiol.-Cell Physiol.* **2022**, *322* (4), C674−C687.
(46) Queisser, K. A.; Mellema, R. A.; Middleton, E. A.; Portier, I.; Manne, B. K.; Denorme, F.; Beswick, E. J.; Rondina, M. T.; Campbell, R. A.; Petrey, A. C. *JCI Insight* **2021**, *6* (17), No. e147472.
(47) Yamaguchi, Y.; Noda, H.; Okaniwa, N.; Adachi, K.; Shinmura, T.; Nakagawa, S.; Ebi, M.; Ogasawara, N.; Funaki, Y.; Zhuo, L.; Kimata, K.; Sasaki, M.; Kasugai, K. *Digestion* **2017**, *95* (2), 146−155.
(48) Rivas, F.; Zahid, O. K.; Reesink, H. L.; Peal, B. T.; Nixon, A. J.; DeAngelis, P. L.; Skardal, A.; Rahbar, E.; Hall, A. R. *Nat. Commun.* **2018**, *9* (1), 1037.
(49) Rivas, F.; DeAngelis, P. L.; Rahbar, E.; Hall, A. R. *Sci. Rep.* **2022**, *12* (1), 4469.
(50) Wei, W.; Faubel, J. L.; Selvakumar, H.; Kovari, D. T.; Tsao, J.; Rivas, F.; Mohabir, A. T.; Krecker, M.; Rahbar, E.; Hall, A. R.; Filler, M. A.; Washburn, J. L.; Weigel, P. H.; Curtis, J. E. *Nat. Commun.* **2019**, *10* (1), 5527.
(51) De Jong, I. E. M.; Hunt, M. L.; Chen, D.; Du, Y.; Llewellyn, J.; Gupta, K.; Li, D.; Erxleben, D.; Rivas, F.; Hall, A. R.; Furth, E. E.; Naji, A.; Liu, C.; Dhand, A.; Burdick, J. A.; Davey, M. G.; Flake, A. W.; Porte, R. J.; Russo, P. A.; Gaynor, J. W.; Wells, R. G. *J. Hepatology* **2023**, *79* (6), p1396.
(52) Michaut, A.; Mongera, A.; Gupta, A.; Serra, M.; Rigoni, P.; Lee, J. G.; Duarte, F.; Hall, A. R.; Mahadevan, L.; Guevorkian, K.; Pourquié, O. *bioRxiv* **2022**, na.
(53) Amargant, F.; Manuel, S. L.; Tu, Q.; Parkes, W. S.; Rivas, F.; Zhou, L. T.; Rowley, J. E.; Villanueva, C. E.; Hornick, J. E.; Shekhawat, G. S.; Wei, J.; Pavone, M. E.; Hall, A. R.; Pritchard, M. T.; Duncan, F. E. *Aging Cell* **2020**, *19* (11), No. e13259.
(54) Fasanello, D. C.; Su, J.; Deng, S.; Yin, R.; Colville, M. J.; Berenson, J. M.; Kelly, C. M.; Freer, H.; Rollins, A.; Wagner, B.; Rivas, F.; Hall, A. R.; Rahbar, E.; DeAngelis, P. L.; Paszek, M. J.; Reesink, H. L. *Arthritis Res. Ther.* **2021**, *23* (1), 218.
(55) Jing, W.; DeAngelis, P. L. *J. Biol. Chem.* **2004**, *279* (40), 42345−42349.
(56) Enghild, J. J.; Thøgersen, I. B.; Pizzo, S. V.; Salvesen, G. *J. Biol. Chem.* **1989**, *264* (27), 15975−15981.
(57) Watkins, A.; Fasanello, D.; Stefanovski, D.; Schurer, S.; Caracappa, K.; D'Agostino, A.; Costello, E.; Freer, H.; Rollins, A.; Read, C.; Su, J.; Colville, M.; Paszek, M.; Wagner, B.; Reesink, H. *BMC Vet. Res.* **2021**, *17* (1), 189.
(58) Clark, S. J.; Keenan, T. D. L.; Fielder, H. L.; Collinson, L. J.; Holley, R. J.; Merry, C. L. R.; van Kuppevelt, T. H.; Day, A. J.; Bishop, P. N. *Investig. Opthalmology Vis. Sci.* **2011**, *52* (9), 6511.
(59) Yang, J.; Ferranti, D. C.; Stern, L. A.; Sanford, C. A.; Huang, J.; Ren, Z.; Qin, L.-C.; Hall, A. R. *Nanotechnology* **2011**, *22* (28), No. 285310.
(60) Wanunu, M.; Dadosh, T.; Ray, V.; Jin, J.; McReynolds, L.; Drndić, M. *Nat. Nanotechnol.* **2010**, *5* (11), 807−814.
(61) Wanunu, M.; Cohen-Karni, D.; Johnson, R. R.; Fields, L.; Benner, J.; Peterman, N.; Zheng, Y.; Klein, M. L.; Drndic, M. *Molecules. J. Am. Chem. Soc.* **2011**, *133* (3), 486−492.
(62) Venta, K.; Shemer, G.; Puster, M.; Rodriguez-Manzo, J. A.; Balan, A.; Rosenstein, J. K.; Shepard, K.; Drndic, M. *ACS Nano* **2013**, *7* (5), 4629−4636.
(63) Carlsen, A. T.; Zahid, O. K.; Ruzicka, J. A.; Taylor, E. W.; Hall, A. R. *Nano Lett.* **2014**, *14* (10), 5488−5492.
(64) Wadsworth, I. D.; Hall, A. R. *Nano Res.* **2022**, *15* (11), 9936−9942.
(65) Wisniewski, H.-G.; Colón, E.; Liublinska, V.; Karia, R. J.; Stabler, T. V.; Attur, M.; Abramson, S. B.; Band, P. A.; Kraus, V. B. *Osteoarthritis Cartilage* **2014**, *22* (2), 235−241.
(66) Mukhopadhyay, D.; Asari, A.; Rugg, M. S.; Day, A. J.; Fülöp, C. *J. Biol. Chem.* **2004**, *279* (12), 11119−11128.
(67) Chang, M. Y.; Chan, C. K.; Braun, K. R.; Green, P. S.; O'Brien, K. D.; Chait, A.; Day, A. J.; Wight, T. N. *J. Biol. Chem.* **2012**, *287* (17), 14122−14135.
(68) Eriksen, G. V.; Carlstedt, I.; Morgelin, M.; Uldbjerg, N.; Malmstrom, A. *J. Biochem.* **1999**, *340* (3), 613−620.
(69) Stefan Lohmander, L.; Neame, P. J.; Sandy, J. D. *Arthritis Rheum.* **1993**, *36* (9), 1214−1222.
(70) Ly, M.; Leach, F. E.; Laremore, T. N.; Toida, T.; Amster, I. J.; Linhardt, R. J. *Nat. Chem. Biol.* **2011**, *7* (11), 827−833.
(71) Buckwalter, J. A.; Rosenberg, L. C. *Protein. J. Biol. Chem.* **1982**, *257* (16), 9830−9839.
(72) Foscarin, S.; Raha-Chowdhury, R.; Fawcett, J. W.; Kwok, J. C. F. *Aging* **2017**, *9* (6), 1607−1622.
(73) Kitagawa, H.; Tsutsumi, K.; Tone, Y.; Sugahara, K. *J. Biol. Chem.* **1997**, *272* (50), 31377−31381.
(74) Im, J.; Lindsay, S.; Wang, X.; Zhang, P. *ACS Nano* **2019**, *13* (6), 6308−6318.
(75) Stern, R.; Jedrzejas, M. J. *Chem. Rev.* **2006**, *106* (3), 818−839.
(76) Thurston, C. F.; Hardingham, T. E.; Muir, H. *Biochem. J.* **1975**, *145* (2), 397−400.
(77) Yamagata, T.; Saito, H.; Habuchi, O.; Suzuki, S. *J. Biol. Chem.* **1968**, *243* (7), 1523−1535.
(78) Colbath, A. C.; Dow, S. W.; Hopkins, L. S.; Phillips, J. N.; McIlwraith, C. W.; Goodrich, L. R. *Front. Vet. Sci.* **2018**, *5*, 208.
(79) Ross, T. N.; Kisiday, J. D.; Hess, T.; McIlwraith, C. W. *Osteoarthritis Cartilage* **2012**, *20* (12), 1583−1590.
(80) Scott, I.; Midha, A.; Rashid, U.; Ball, S.; Walding, A.; Kerry, P.; Delaney, S.; Cruwys, S. *Osteoarthritis Cartilage* **2009**, *17* (6), 790−797.
(81) Nelson, B. B.; King, M. R.; Frisbie, D. D. *Vet. J.* **2017**, *229*, 54−59.
(82) Band, P. A.; Heeter, J.; Wisniewski, H.-G.; Liublinska, V.; Pattanayak, C. W.; Karia, R. J.; Stabler, T.; Balazs, E. A.; Kraus, V. B. *Osteoarthritis Cartilage* **2015**, *23* (1), 70−76.

https://doi.org/10.1021/acs.analchem.3c04387
Anal. Chem. XXXX, XXX, XXX−XXX